

Miniaturized HMSIW Dual-Band Filter Based on CSRRs and Microstrip Open-Stubs

Dan-Dan Lv, Ling-Qin Meng*, and Zhe Zou

Abstract—A method is proposed for a half-mode substrate integrated waveguide (HMSIW) bandpass filter (BPF) to obtain dualband below the cutoff frequency. Complementary split-ring resonators (CSRRs) and microstrip open-stubs are integrated on the top of an HMSIW cavity. The structure produces two center frequencies both below the cutoff frequency of the original HMSIW without increasing the cavity size. Results indicate that the center frequencies are 2.95 GHz and 3.99 GHz, and 3 dB fractional bandwidths (FBWs) are 9.1% and 4.6%, respectively. There is a transmission zero between the two frequencies, which enhances the out-of-band suppression performance. The measured results are in good agreement with the simulated ones. This new combination not only obtains two usable passbands below the cutoff frequency, but also makes the filter more compact. The filter has some practical and application significance.

1. INTRODUCTION

Filters have always been an indispensable part in microwave and millimeter wave systems, and their performances affect the communication quality of the whole system [1]. Traditional metal waveguides are bulky and difficult to integrate with the planar structures. Coplanar waveguides have a lower frequency selectivity because of their low quality factor. To overcome these disadvantages, Substrate Integrated Waveguide (SIW) has been introduced.

SIW is made with a pair of periodic metalized via arrays or slot trenches. This emerging guided-wave structure looks like two parallel fences that have a specific spacing in which EM waves are well confined. The position and size of the holes on the HMSIW cavity can adjust the resonant frequency point and filter performance [2]. [3] proposed a new type of substrate integrated waveguide filter with periodic holes arranged in a circular shape, and this filter operates at 20 GHz. An SIW bandpass filter combined with other structures can enhance transmission band characteristics by introducing transmission zeros, for example, SIW with an electromagnetic band gap (EBG) structure in [4], E-shape defected ground structure (DGS) in [5] or metamaterial structures in [6], but these methods will make production complicated. U groove is etched on the surface of the cavity [7], and the CSRR is loaded at the bottom to reduce the filter size [8]. A substrate loaded integrated waveguide dual pass filter with dual capacitor loading is shown in [9]. The size can be reduced, but the operation is complex and difficult to implement.

SIW inherits the advantages of traditional waveguide devices. Besides, it is cheap and easy to fabricate. So HMSIW and quarter-mode substrate integrated waveguide (QMSIW) are now widely used. QMSIW and CSRR are combined to realize dual-band filter in [10].

Based on an HMSIW cavity, symmetrical CSRRs and microstrip open-stub are added to the HMSIW cavity to generate resonance at 2.95 and 3.99 GHz, respectively. As we all know, the smaller the HMSIW filter size is, the higher the cutoff frequency is. This method does not increase the size, but

Received 2 March 2018, Accepted 28 June 2018, Scheduled 20 July 2018

* Corresponding author: Ling-Qin Meng (menglq@shu.edu.cn).

The authors are with the Key Laboratory of Specialty Fiber Optics and Optical Access Network, Shanghai University, Shanghai 200072, China.

has two passbands below the cutoff frequency without increasing the size of the cavity. The proposed filter not only inherits the advantages of traditional SIW filters, but also has the characteristics of miniaturization and low cost. The utility model has the feasibility of being applied to various microwave and millimeter wave devices.

2. ANALYSIS AND DESIGN OF FILTER

2.1. HMSIW-CSRRs Filter

Studies show that there is apoptosis wave in the part below the working frequency of waveguide. These apoptosis waves are supposed to decay rapidly from the source of excitation and cannot be transmitted to the other end of the waveguide. Etching a resonant ring structure on the surface of substrate integrated waveguide can amplify the apoptosis wave and generate deep out-of-band inhibition near the resonant frequency. In this paper, CSRRs are etched into HMSIW cavity to form a new passband below the cutoff frequency, which is equivalent to miniaturization.

The CSRR unit is shown in Fig. 1(a), in which white represents slots, and the rest is metal. When the CSRR is loaded on HMSIW, it is usually equalized as a parallel circuit formed by a capacitor and an inductor. If the gap d is not negligible with respect to side length a , the equivalent inductance L_{s1} and equivalent capacitance C_{s1} of CSRR are calculated by the following formulas.

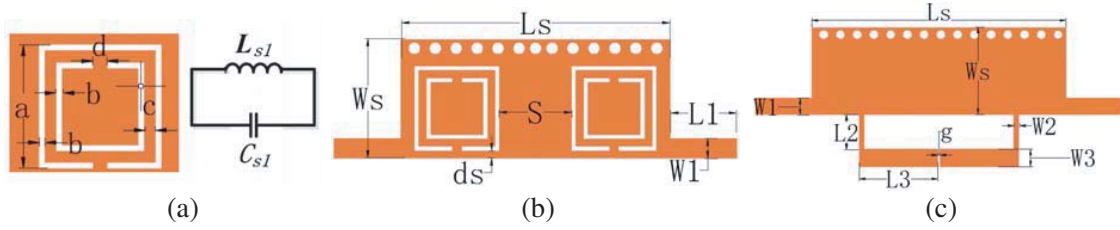


Figure 1. (a) The CSRR unit and its equivalent circuit. (b) Top view of HMSIW-CSRRs filter. (c) Top view of HMSIW-microstrip open-stubs filter.

Equivalent inductance of CSRR:

$$L_{s1} = \frac{\mu_0 a}{2\pi} \left[\ln \left(\frac{2a}{b+t} \right) + 0.5 - \frac{b^2 + t^2}{24a^2} + \sqrt{\frac{b^2 + t^2 + 0.46bt}{3a}} \right] \quad (1)$$

Equivalent capacitance of CSRR:

$$C_{s1} = [3.5 \times 10^{-5} \times 1.9t (R_{out} + R_{in})] \quad (2)$$

wherein t is the thickness of metal, and R_{out} refers to the inner tangential radius of CSRR outer ring, while R_{in} refers to the inner tangential radius of inner ring.

The resonant frequency of the CSRR is:

$$f_{s1} = \frac{1}{2\pi\sqrt{L_{s1}C_{s1}}} \quad (3)$$

SIW waveguide is a microstrip structure. When the substrate is thick, the radiation is large, which is not conducive to energy transmission. The ratio of structural size to substrate thickness is usually large, so HMSIW can be seen as inserting a perfect magnetic wall into the center of the longitudinal axis of SIW. The upper and lower structures of the waveguide are symmetrical, which will not cause too much leakage, but will lead to increased total inductance. The outer ring opening faces the magnetic wall, which is mainly reflected by magnetic field coupling, so the resonant frequency moves to the low frequency. As the distance d_s between the opening of the outer ring and the magnetic wall increases, the frequency will move to the low frequency. The inner and outer ring spacing c is decreased, and increased mutual inductance between them leads to increased coupling. The frequency will also move

to the low frequency. In the whole design process, the CSRR structure remains the same, and the total capacitance C_{S1} is only related to R_{out} and R_{in} , so the capacitance value is regarded as the same.

In Fig. 1(b), symmetric CSRRs are adopted to better amplify the apoptosis wave and optimize the passband characteristics, but the adjacent resonant rings will generate mutual inductance. The spacing S between the two rings decreases, and the enhancement of mutual inductance leads to the enhancement of magnetic field coupling. The space between the two resonant points in the passband is increased, and the corresponding bandwidth is widened, but the performance will be sacrificed.

According to the above analysis, the parameters of HMSIW-CSRRs filter are determined by simulation and optimization: $L_s = 18$, $W_s = 8$, $s = 4.8$, $ds = 0.3$, $L_1 = 4.6$, $W_1 = 1.2$, $a = 5.9$, $b = 0.3$, $c = 0.5$, and $d = 0.6$ (unit: mm). The simulated S -parameters of HMSIW-CSRRs filter and HMSIW are shown in Fig. 2(a). The cutoff frequency of HMSIW is 7.8 GHz. In addition, we get a new passband at 3.18 GHz, in which the working frequency is reduced by 59.2%, equivalent to miniaturization. The 3 dB bandwidth is from 3.02 to 3.34 GHz, and the 3 dB fractional bandwidth is 10%. The return loss is better than 36 dB in the passband.

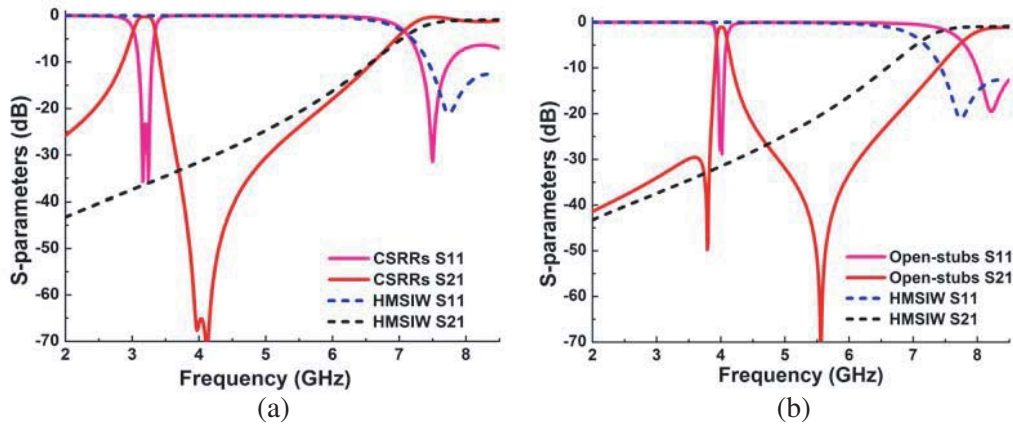


Figure 2. Simulated results of the two filters are compared with HMSIW. (a) HMSIW-CSRRs filter. (b) HMSIW-microstrip open-stubs filter.

2.2. HMSIW-Microstrip Open-Stubs Filter

Symmetric microstrip open-stubs are added to original HMSIW. Fig. 1(c) shows the structure of the proposed filter. When working in resonant state, the microstrip open-stubs are equivalent to a quarter of a wavelength resonator, whose resonant frequency can be approximately derived by equation:

$$f_{s2} \approx \frac{c}{4(L_2 + L_3) \sqrt{\varepsilon_{eff}}} \quad (4)$$

where c is the speed of light in free space; L_2 and L_3 are the physical length of microstrip open-stub lines, respectively.

$$\varepsilon_{eff} = \frac{\varepsilon_r - 1}{2} + \frac{\varepsilon_r + 1}{2} \left[\left(1 + 24 \frac{h}{w_2 + w_3} \right)^{-1/2} + 0.04 \left(1 - \frac{w_2 + w_3}{2h} \right)^2 \right] \quad (5)$$

where ε_{eff} is the effective dielectric constant, ε_r the relative dielectric constant of the substrate, and h the thickness of substrate

Thus, the center frequency of the passband can be obtained by Equations (4) and (5), and can be controlled by changing the values of L_2 and L_3 .

According to analysis and optimization, the parameters are determined: $L_s = 20$, $W_s = 8$, $L_1 = 4.9$, $W_1 = 1.4$, $L_2 = 3$, $W_2 = 0.5$, $L_3 = 6.6$, $W_3 = 1$, and $g = 0.2$ (unit: mm). As can be seen from Fig. 2(b), another passband is implemented. The structure produces a passband at 4.0 GHz with 3 dB bandwidth from 3.88 to 4.12 GHz and a 3 dB fractional bandwidth of 6.0%. The return loss is better than 28 dB in the passband. Two transmission zeros are introduced to the filter. The filter has high selectivity and high suppression.

2.3. Dual-Band Filter Design

As analyzed above, a dual-band filter is designed by integrating CSRRs and microstrip open-stubs. Configuration of the dual-band HMSIW filter is shown in Fig. 3. The geometrical parameters are: $L_s = 18$, $W_s = 7.5$, $L_1 = 4.6$, $W_1 = 1.3$, $L_2 = 3$, $W_2 = 1$, $L_3 = 6.4$, $W_3 = 0.5$, $s = 4$, $ds = 0.5$, $a = 5.7$, $b = 0.3$, $c = 0.5$, and $d = 0.6$ (unit: mm).

This filter consists of the symmetric CSRRs, symmetric microstrip open-stubs and HMSIW transmission lines. The $50\ \Omega$ microstrip lines are directly connected to the cavity at input/output ports. It is worth mentioning that the combination of CSRRs and microstrip open-stubs is equivalent to increasing the distance d_s between the opening of the outer ring and the magnetic wall, resulting in the increase of inductance. The combination will affect the passband, and the frequency may be reduced.

The fabricated filters are shown in Fig. 4. They are fabricated on an RO5880 substrate ($\epsilon_r = 2.2$, $\tan \delta = 0.0009$). The substrate size of the dual-band filter is $0.26\lambda_g \times 0.14\lambda_g$ (λ_g represents the guided wavelength at the center frequency of the first passband). The fabricated filters were measured by an Agilent 8722ES network analyzer.

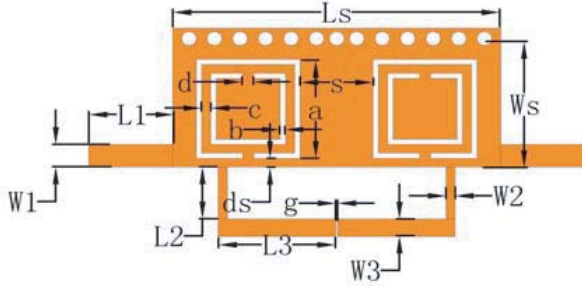


Figure 3. Top view of the proposed dual-filter.

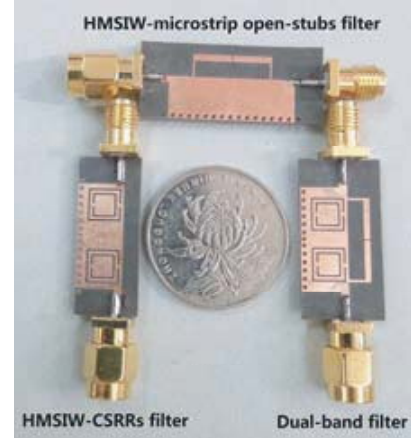


Figure 4. Photograph of fabricated filters.

3. EXPERIMENT RESULTS AND DISCUSSION

The surface electric field distribution is shown in Fig. 5. The simulated and measured results of the HMSIW-CSRRs filter and HMSIW-microstrip open-stubs filter are shown in Fig. 6(a) and Fig. 6(b). The first passband is produced by CSRRs, and the second passband is generated by the microstrip open-stubs. This is also better illustrated by the surface electric field distribution. We can see that the return loss of the first pass band is worse than that of the simulated result, and other properties are consistent. For example, the center frequency is not offset, and the bandwidth is as wide as in the simulation result. However, the second passband not only has higher return loss than the simulated result, but also has a much narrower bandwidth. This is because the open microstrip is an open structure. Its ability to bind energy is weaker than the CSRR structure, and energy in the microstrip open-stubs is more likely to leak. So the second passband is more sensitive to manufacturing dispersions while there are dimensional errors in fabrication. The ripple is a systematic error of the network analyzer. Especially, the frequency is greater than 5.0 GHz, and the loss of the connector is greater, so the high frequency jitter in the test result is more obvious.

The simulated and measured results of the dual-band filter are substantially consistent in Fig. 6(c). The measured center frequencies of the dual-band filter are 2.95 and 3.99 GHz, with 3 dB fractional bandwidths of 9.1% and 4.6%, respectively. The minimum insertion losses are 0.9 and 1.48 dB, while

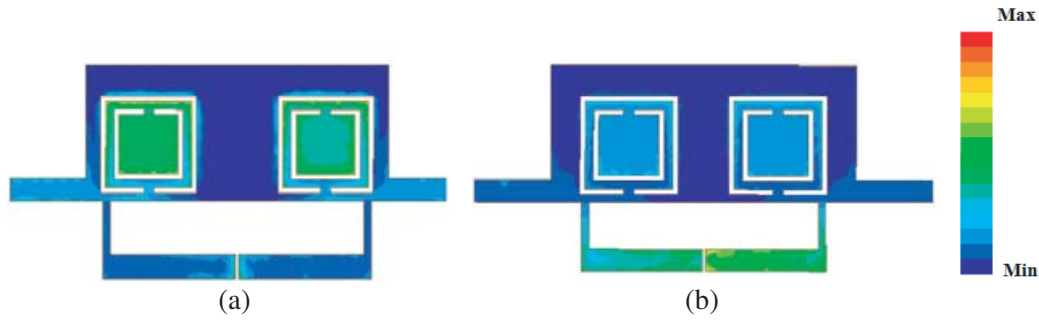


Figure 5. The surface electric field distribution of dual-band filter at each frequency point. (a) 2.95 GHz, (b) 3.99 GHz.

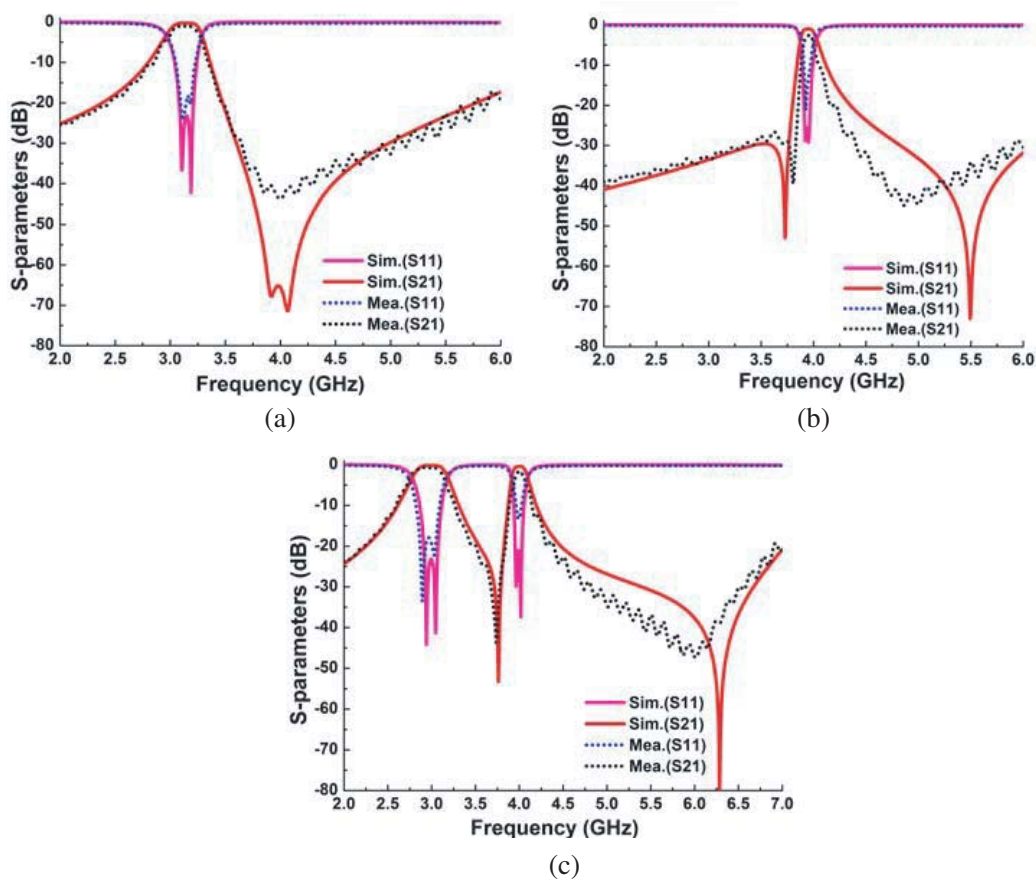


Figure 6. Simulated and measured results of (a) HMSIW-CSRRs filter, (b) HMSIW-microstrip open-stubs filter, (c) dual-band filter.

the return losses are all better than 15 dB. There is a transmission zero between the passbands, providing a stopband with the rejection better than 45 dB. Compared with the first band of the dual-band filter, the center frequency of the HMSIW-CSRRs filter is reduced from 3.18 to 2.95 GHz. It is because d_s is increased, resulting in the increase of inductance, so the frequency is reduced.

Here, some comparisons are summarized in Table 1. The filter in [8] has a similar size, and the frequencies are higher than the proposed filter. The center frequencies of the filters are similar in [9] and [10] but larger than the proposed filter. It can be seen that the proposed dual-band BPF has two lower frequencies, two reasonable bandwidths and smaller size.

Table 1. Comparison of the proposed filter with some references.

Reference	Center frequencies (GHz)	Fractional bandwidths(%)	Size ($\lambda_g \times \lambda_g$)	Technology
[2]	4.91/6.88	1.6/2.0	1.0×1.0	SIW-LTCC
[8]	5.0/7.5	3.0/4.2	0.28×0.27	SIW-CRLH and CSRRs
[9]	2.51/5.3	6.8/5.8	0.84×0.42	SIW-dual-capacitively
[10]	3.5/5.7	3.3/6.4	0.5×0.5	QMSIW-CSRRs
This work	2.95/3.99	9.1/4.6	0.26×0.14	HMSIW-CSRRs and microstrip openstubs

4. CONCLUSION

An approach to design the miniaturized dual-band HMSIW filter is proposed. Center frequencies are controlled by the CSRRs and microstrip open-stubs. They are below the cutoff frequency of the HMSIW and avoid increasing the size. After simulation and optimization, the proposed filter is fabricated and measured. The results show that two center frequencies are 2.95 and 3.99 GHz with 3 dB fractional bandwidths of 9.1% and 4.6%. The transmission zero enhances the out-of-band suppression performance. Such a dual-band HMSIW filter has good performance and is feasible in engineering.

REFERENCES

1. Wang, Z., T. Yang, and J. Dong, "A compact triple-mode bandpass HMSIW filter," *Progress In Electromagnetics Research Letters*, Vol. 48, 39–43, 2014.
2. Cheng, F., X. Q. Lin, X. X. Liu, et al., "A compact dual-band bandpass SIW filter," *Journal of Electromagnetic Waves and Applications*, Vol. 27, No. 3, 338–344, 2013.
3. Wei, Q. F., Z. F. Li, L. S. Wu, et al., "A novel multilayered cross-coupled substrate-integrated waveguide (SIW) circular cavity filter in LTCC," *Microwave & Optical Technology Letters*, Vol. 51, No. 7, 1686–1689, 2009.
4. Li, D., C. M. Tong, J. S. Bao, et al., "A novel bandpass filter of Substrate Integrated Waveguide (SIW) based on S-shaped EBG," *Progress In Electromagnetics Research Letters*, Vol. 36, 191–200, 2013.
5. Xu, S., K. Ma, F. Meng, et al., "Novel defected ground structure and two-side loading scheme for miniaturized dual-band SIW bandpass filter designs," *IEEE Microwave & Wireless Components Letters*, Vol. 25, No. 4, 217–219, 2015.
6. Baena, J. D., J. Bonache, F. Martin, et al., "Equivalent-circuit models for split-ring resonators and complementary split-ring resonators coupled to planar transmission lines," *IEEE Transactions on Microwave Theory & Techniques*, Vol. 53, No. 4, 1451–1461, 2005.
7. Chen, R. S., S. W. Wong, L. Zhu, et al., "Wideband bandpass filter using U-slotted Substrate Integrated Waveguide (SIW) cavities," *IEEE Microwave & Wireless Components Letters*, Vol. 25, No. 1, 1–3, 2015.
8. Zhao, Q., Z. Chen, J. Huang, et al., "Compact dual-band bandpass filter based on composite right/left-handed substrate integrated waveguide loaded by complementary split-ring resonators defected ground structure," *Journal of Electromagnetic Waves & Applications*, Vol. 28, No. 14, 1807–1814, 2014.
9. Li, M., C. Chen, and W. Chen, "Miniaturized dual-band filter using dual-capacitively loaded SIW cavities," *IEEE Microwave & Wireless Components Letters*, Vol. 99, 1–3, 2017.
10. Wang, K., H. Tang, R. Wu, et al., "A novel compact dual-band filter based on quarter-mode substrate integrated waveguide and complementary split-ring resonator," *Microwave & Optical Technology Letters*, Vol. 58, No. 11, 2704–2707, 2016.